Journal of Cluster Science (2019) 30:687–705
https://doi.org/10.1007/s10876-019-01528-5

ORIGINAL PAPER

Potential Nematicidal Properties of Silver Boron Nanoparticles: Synthesis, Characterization, In Vitro and In Vivo Root-Knot Nematode (*Meloidogyne incognita*) Treatments

Ahmed I. El-Batal[1] · Mohamed S. Attia[2] · Mohamed M. Nofel[2] · Gharieb S. El-Sayyad[1]

Received: 31 January 2019 / Published online: 13 March 2019

Abstract

The purpose of this work is to evaluate the anti-nematode activity of silver boron nanoparticles (AgB NPs) synthesized by PVP polymer and gamma rays as a novel cost-effective and eco-friendly green method. AgB NPs were structurally identified by UV–Vis., XRD, HRTM, DLS, FTIR, SEM and EDX mapping analysis. A suggested reaction mechanism was considered. In-vitro and in vivo nematicidal potential of AgB NPs against root-knot *Meloidogyne incognita* was examined. HRTEM image exhibited spherical AgB NPs with a diameter of 29.55 nm. FTIR spectrum explains that there is a continuous reduction of ions due to PVP oxidation. AgB NPs possesses an encourage anti-nematode against *M. incognita* causing root-knot in the tomato plant. Treatment 3 exhibited the maximum mortality as 74.20% after 96 h. It also decreased root galls and egg masses numbers after 1 week of the infection (20.33 galls and 2.33 egg masses). Treatments 3 and 4 reduced the numbers of the 2nd stage juveniles, females and the developmental stages. Boron at the permissible limits was adjusted to be more than silver in the synthesized AgB NPs (to avoid the toxicity) for developing the resistance and immunity of the tomato plant. Therefore, AgB NPs may recognize potential targets within agricultural treatments.

Keywords Root-knot nematode · PVP · Anti-nematode · Silver boron nanoparticles · Gamma irradiation

Introduction

Nematode-infected some plants are amongst the principal and basic soil-borne pathogens and are regarded as a menace to the agricultural fields because they generate a root disease in most of the vegetables and fruits. As a response of nematode infection, seasonal yield declines in all crops are determined to be about 75.0 billion USD [1, 2]. The numbers of nematode species which harm to all crops were calculated to be about 4000 species [3].

Nematode-mediated root-knot is considered to be the common agricultural insects around the world and in a distinct, *Meloidogyne incognita* is supposed to be the general economically significant insect [4, 5]. They have spoiled every piece of the plant such as roots, leaves, stems, rhizomes, buds, bulbs, seeds and flowers [3]. The mechanism of *M. incognita* infection starts with the attacking of the 2nd stage juveniles through the crop roots. They moved over the plant tissue and produce strong feeding section which described as the giant holes that

✉ Gharieb S. El-Sayyad
Gharieb.Elsayyad@eaea.org.eg; adham_adham699@yahoo.com

Ahmed I. El-Batal
Ahmed.Elbatal@eaea.org.eg; aelbatal2000@gmail.com

Mohamed S. Attia
drmohamedsalah92@azhar.edu.eg; drmohamedsalah92@yahoo.com

Mohamed M. Nofel
mohamed_mahmud21@yahoo.com

[1] Drug Radiation Research Department, Biotechnology Division, National Center for Radiation Research and Technology (NCRRT), Atomic Energy Authority, Cairo, Egypt

[2] Botany and Microbiology Department, Faculty of Science, Al-Azhar University, Nasr City, Cairo 11884, Egypt

decrease the ability of water transportation and the nutrient absorption in the infected crops [6].

The environmental constraint regarding the use of the synthetic chemicals and the biological control [5], which possesses a nematicidal potential to invade *M. incognita* were encouraged, so nano-materials have become a developing concern. Although some researches were conducted Ag NPs as an anti-nematode agent, there is still a demand for the substitutional nano-composite not only for the adequate *M. incognita* restriction but also stimulate the plant growth and increasing the crops immunity [7, 8].

Nanotechnology seems to be the novel idea of science and technology across the world with the materials possesses a unique nano-scale [9, 10]. There is a continuous trying for developing new methods regarding novel nano-materials with unique characteristics for different and important applications. It may be included carbon-based elements (nano-tubes), metal-based particles (Ag NPs or Au NPs) or nano-composites (mixed NPs having diverse features) [11].

The study towards inorganic–polymer nano-composite has achieved vital consideration due to the novelty in their property that initiated following the reaction within inorganic salts and polymer elements. The resultant nano-composites were conducted in various fields such as cosmetics, optoelectronics, agricultural and biomedical applications [12].

In the last years, there is a memorable synthesis of several nano-composites and diverse new procedures [13, 14] were designed for the development of novel nano-composites with necessary features and objects like the mechanical mixing, biological production, gamma rays-assistant nucleation and the sol–gel procedure. In order to control the construction of inorganic–polymer NPs, the organic polymeric substances like PVA and PVP (as a stabilizing agent) were connected and mixed with different metal salts throughout the capping method [15].

The unique shape, size, morphological appearance and different arrangements which founded in the synthesized nano-composite were excellent consideration which in terms were advanced the catalytic, opto-electric and visible features [16–18]. It must be noted that different NPs were synthesized by various synthetic methods like biological, physical and chemical processes [19–23]. Between the physical process, gamma rays were established to be an available practice for NPs production which needs an aqueous solution at room temperature [24–26].

Different NPs like Ag NPs were applied for diverse purposes e.g. in pharmaceutical supplies, ultra-thin silicon solar cell processing, an additive in the laundry machines and smart antimicrobial agent [27–30]. Between the agricultural application, Ag NPs were supported in the latest few years as a pesticide to manage the invasion of the plant pathogen such as root-knot nematode [1, 3, 31, 32].

Boron is a required nutrient for the germination and the improvement of normal crops [33]. It was utilized as a micronutrient (in small addition) which include a mean function as a fertilizer [33, 34]. But when applied in extensive concentrations, it functioned as algaecides, anti-herbal agent and pesticides (as in our study) for root-knot nematode [35, 36].

Boron performs an important function in the catalytic process [37], and in a different area of crops functions like cell wall structure and resistance, supporting of the basic and the operative solidity of the living membranes, the flow of sugar or power toward the developing portions of crops and seed collection. Sufficient boron is further wanted for efficient nitrogen fixation and nodulation of roots in the legume plants [3, 33–35, 38].

In this regard, we decided for the first time, PVP (capping and stabilizing polymer), as a prototype to design a promising cost-efficient and eco-friendly green synthesis of AgB NPs following the influence of gamma rays. A complete validation and description had been done to gain more advanced data regarding the size, crystallinity, distribution, and appearance of the combined AgB NPs. After that, the research of both in vitro and in vivo anti-nematode potential of AgB NPs against *M. incognita*-mediated root-knot nematode were tested.

Materials and Methods

Reagents and Chemicals

Media components were obtained from (Oxoid) and (Difco). Chemicals utilized (silver nitrate, boric Acid, sodium hypochlorite, PVP, and isopropyl alcohol) and reagents were taken as standard materials (Sigma-Aldrich).

Gamma Radiation Source

Gamma radiation process was conducted at the NCRRT, Cairo, Egypt. The used source was ^{60}Co-Gamma chamber 4000-A-India. Gamma rays were presented as ^{60}Co gamma rays (dose rate; 2.10 kGy/h). In this way, ^{60}Co gamma rays were reacted with the prepared solutions to create the hydrated free electrons after water radiolysis.

Synthesis and Incorporation of Silver Boron Nanoparticles

AgB NPs were synthesized by PVP as a stabilizing agent and gamma radiation as a reducing agent. The prepared mixture solution contained 1.0 ml (100 mM) boric acid

and 1.0 ml (100 mM) silver nitrate and completed to approximately 25.0 ml of PVP (4.0%) and isopropyl alcohol (0.2%; free radical scavenger) solution. The prepared mixtures were gamma irradiated at different gamma doses (10.0, 15.0, 20.0, and 25.0 kGy). The most efficient gamma rays dose was determined following the estimation of the Optical Density (O.D.) by UV–Vis. spectroscopy.

The optimization experiment was investigating the impact of the concentration of silver nitrate and boric acid regarding AgB NPs synthesis after displaying to the most potent gamma rays. The measured factors were included two variables in six levels (the concentration of silver nitrate and boric acid).

Various concentration of silver nitrate solution (2.0, 4.0, 6.0, 8.0, 10.0 and 12.0 mM) were associated with different boric acid concentration (2.0, 4.0, 8.0, 12.0, 16.0 and 20.0 mM). Every experiment was completed by adding 0.2% isopropyl alcohol and 4.0% PVP. After that, all the prepared solutions were stirred at room temp, (25.0 ± 1.0 °C) and then displayed to the most effective gamma dose. Finally, the most optimized run was chosen according to the highest O.D. (High yield) which estimated following the UV–Vis. investigation.

Characterization of Silver Boron Nanoparticles

X-Ray Diffraction (XRD) was applied to define the crystallinity and crystallite size/lattice strain elements. It was combined with the XRD-6000 lists, Shimadzu apparatus, SSI, Japan. The intensity of the diffracted X-rays estimated the diffracted angle 2θ. FT-IR study was a vital target that gives information regarding the chemical functional groups remaining in PVP. The experiments were carried out through a JASCO FT-IR 3600 Infra-Red spectrometer within KBr process. It was confirmed at a wave number range from 400 to 4000 cm^{-1}. The synthesized AgB NPs was characterized by UV–Visible spectrophotometer throughout JASCO V-560. UV–Vis. Spectrophotometer comparing a negative controls (the irradiated samples without salts; for auto-zero support).

Additionally, the average particle size distribution of the synthesized AgB NPs was defined through Dynamic Light Scattering DLS-PSS-NICOMP 380-USA. Also, the synthesized AgB NPs common size and actual shape were recorded by using High-Resolution Transmission Electron Microscope (HRTEM) JEM2100, Jeol, Japan. The surface morphology and the distribution of Ag and B in the synthesized AgB NPs and PVP were examined via Scanning Electron Microscopy (SEM) EM, ZEISS, EVO-MA10, Germany. Finally, Energy-dispersive X-ray (EDX) BRUKER, Nano GmbH, D-12489, 410-M, Germany was utilized to estimate the elemental composition and the mapping method (with the aid of SEM) for giving a complete knowledge regarding the purity of the synthesized AgB NPs.

Tomato Plant Seedlings

The Tomato plant seedlings (*Lycopersicon esculentum*; 4 weeks old) were taken kindly from Agricultural Research Center (ARC), Giza, Egypt at the beginning of April 2018.

Preparation of Root-Knot Nematode Inoculums

The culture of root-knot nematode (*Meloidogyne incognita*) was collected from a particular egg mass of the adult females and distinguished by the morphological features of the female original as reported by Taylor and Sasser [39].

The eggs of root-knot nematode were derived from the known tomato roots by sodium hypochlorite (NaOCl; 0.5%) solution as defined by Hussey and Barker [40]. The prepared roots were sliced into small parts and then macerated toward two periods of 10 s (at raised velocity applying an electric blender). The system delivered the largest number of nematodes from sources. After that, the obtained macerated root extract was stored within a one litre conical flask including the NaOCl solution.

In order to deliver the eggs from the gelatinous form, the prepared solution was quickly agitated for 3.0 min. After that, the collected solution was discharged within several size sieves to separate root tissue. It must be mentioned that eggs were received near 20.0 μm (635.0 meshes) sieve and cleaned many times with tap water to eliminate the residual of NaOCl used, as displayed in Fig. 1. The received eggs were kept in a flask including tap water then investigated under a light microscope. Additionally, root-knot nematode inoculums were fixed at about 20.0 ± 1 juvenile/ml.

Preparation of Silver Boron Nanoparticle Treatments

In the present experiment, we prepared a total of five treatments in order to determine the nematicidal potential of these treatments. The treatments were conducted as silver to boron elemental ratio as mentioned in Table 1. The purpose of the treatments preparation (as the specific ratio) was to determine the effect of both silver and boron ratio on the nematode infection following the specific treatment.

As obtained in Table 1, we have chosen the silver ratio more than boron ten times as in the treatment 1 and vice versa in the treatment 4. On the other hand, the silver: boron ratio in both treatments 2 and 5 was equal but the concentration of both in treatment 5 more than 2. Finally, treatment 3 contains boron elemental ratio more than silver

Fig. 1 A simple scheme represented the extraction methods of nematode juveniles

Table 1 Treatments used in anti-nematode experiment and its corresponding silver and boron elemental ratio

Treatments	Conc. of silver nitrate (mM)	Conc. of boric acid (mM)	Ag:B element ratio
1	1.0	1.0	10:1
2	0.2	2.0	1:1
3	0.1	4.0	1:4
4	0.1	10.0	1:10
5	1.0	10.0	1:1

4 times to determine the effect of boron at a high concentration more than silver.

Laboratory Experiment: Nematode Juveniles Mortality (In Vitro Study)

In this trial, three various concentrations (100.0, 50.0 and 25.0%) of all the treatments (Table 1) of the synthesized AgB NPs were associated with *M. incognita* 2nd stage juveniles (1:1 v/v) to define their influence on the nematode juvenile's mortality. About 3.0 ml of the freshly prepared juvenile's suspension (about 20.0 juveniles/ml) and 3.0 ml of each treatment (Table 1) with their concentration were carried out within sterile Petri dishes (5.0 cm in diameter). Additionally, every treatment was replicated three times. Finally, a control one was applied which contains distilled water instead of the treatments.

On the other hand, all the Petri dishes were incubated for varying four times like 24.0, 48.0, 72.0 and 96.0 h and the number of inactive juveniles was defined supporting the low power stereomicroscope (10×) then the mortality percentage was determined. The treatments activity was evaluated as the inactive nematodes percentage. Also, the three states were examined (2nd juvenile, 3rd, 4th juveniles and adult female of the root-knot nematode; Fig. 2) to assess the actual nematode juvenile's mortality.

Greenhouse Experiment (In Vivo Study)

The tomato plant seedlings were transplanted to a distinct plastic pot (20.0 cm diameter) which supplied with autoclaved sandy clay soil and received only one tomato plant. The five treatments (Table 1) were provided three times. The first treatment was involved at 1 week before the inoculation with *M. incognita* (2000; 2nd stage juveniles) while the second one was involved at the same time of the inoculation and the third treatment was used at 1 week after the inoculation.

On the other hand, five tomato plastic pots were inoculated with 2000 2nd stage juveniles of *M. incognita* and without any treatments. Also, five tomato plastic pots were left without any treatment or infection with *M. incognita* which assisted as controls. All the treatments were replicated five times and were prepared in a full randomized block pattern. Also, all pots were maintained in the greenhouse (at 25.0 ± 5.0 °C) which supplied with the necessary water and the normal nutrient solutions.

After 2 months of the nematode injection, tomato plant seedlings were particularly removed and then roots were

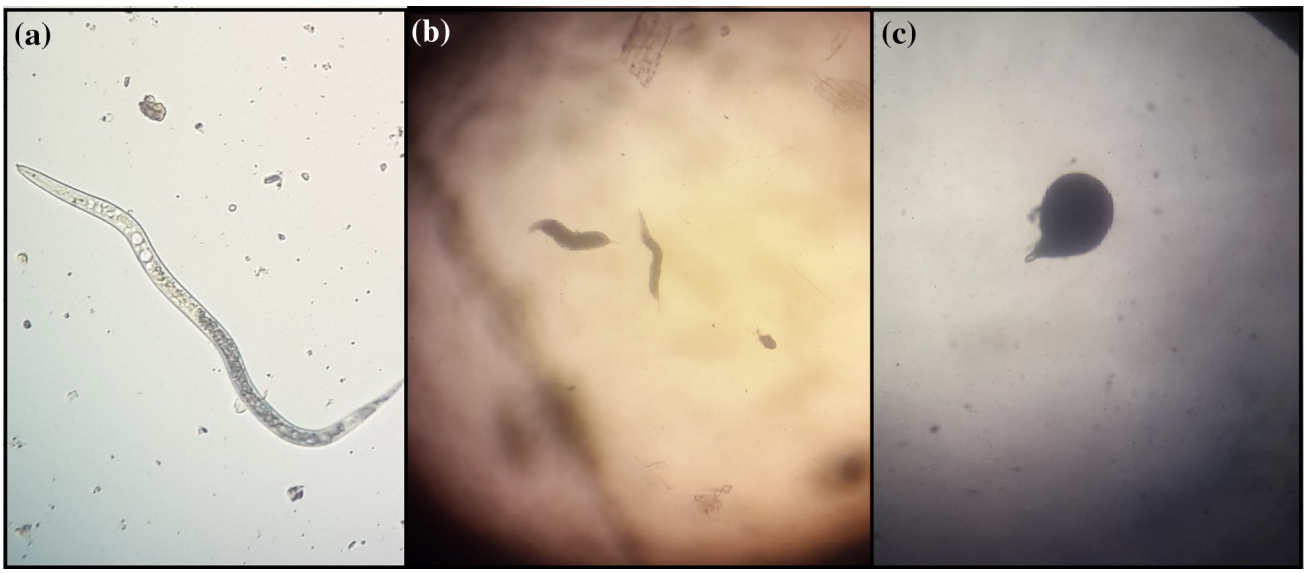

Fig. 2 Nematode juveniles mortality where **a** 2nd juvenile, **b** 3rd and 4th juveniles and **c** adult female of the root knot nematode, *Meloidogyne incognita*

cleaned to discharge the soil and root-knot nematode galls and egg sections were calculated per 1.0 g roots which stained within phloxine B. Reduction percentages (Red. %) of the root-knot nematode galls numbers, egg blocks numbers, 2nd stage juveniles, adult female numbers and the developmental stage numbers were calculated in association with the prepared controls.

Statistical Analysis

The statistical studied of the results were implemented by applying the ONE WAY ANOVA (at $P < 0.05$), Duncan's multiple ranges and the least significant difference summary (LSD) [41]. The results and data were examined and calculated by SPSS software version 15.

Results and Discussion

Synthesis of AgB NPs by PVP and Gamma Rays

As represented in Fig. 3a and Table 2 the actual and active gamma dose which conducted for AgB NPs synthesis was determined to be at 20.0 kGy with the raised O.D. about 0.7780 which diluted 15 times at a specific wavelength 420.0 nm.

Table 3 confirmed AgB NPs synthesis by the reduction of silver nitrate and boric acid solutions (both at different concentrations) after mixing with a stabilizing agent solution (4.0% PVP) and exposed to 20.0 kGy gamma radiation (a reducing agent).

The result shown in Table 3 displayed that, the most accepted run which holding high yield about 2.890 (which diluted 15 times) for AgB NPs production was run 5 which consists of 16.0 mM boric acid and 4.0 mM silver nitrate at 410.0 nm wavelength. Additionally, Fig. 3b represents the continuous O.D. expanding among the first runs (runs 1–5; Table 3) where silver nitrate concentration was fixed at 4.0 mM and boric acid concentration was changed from 2.0 to 16.0 mM. It must be noted that O.D. was declined in the run 6 when the boric acid concentration was at 20.0 mM. On the other hand, Fig. 3b shows that there is steadily increasing in the O.D with the second runs (runs 7–12; Table 3) where boric acid concentration was fixed at 4.0 mM and silver nitrate concentration was varied from 2.0 to 12.0 mM. Both runs 11 and 12 in Table 3 are equivalent in the O.D. but there are changing (red-shift) in the wavelength in the run 12 to the high wavelength which giving the extended size in AgB NPs. Therefore, we do not require to increase the concentration of silver nitrate to give the highest yield.

Results obtained in Table 3 and Fig. 3b displays that the O.D. of AgB NPs develops the peak intensities with simultaneous blue shifts. This means the production of AgB NPs with greater yields and small size [42]. It is notably recognized that AgB NPs solutions display a dark brownish appearance due to the Surface Plasmon Resonance (SPR) [43].

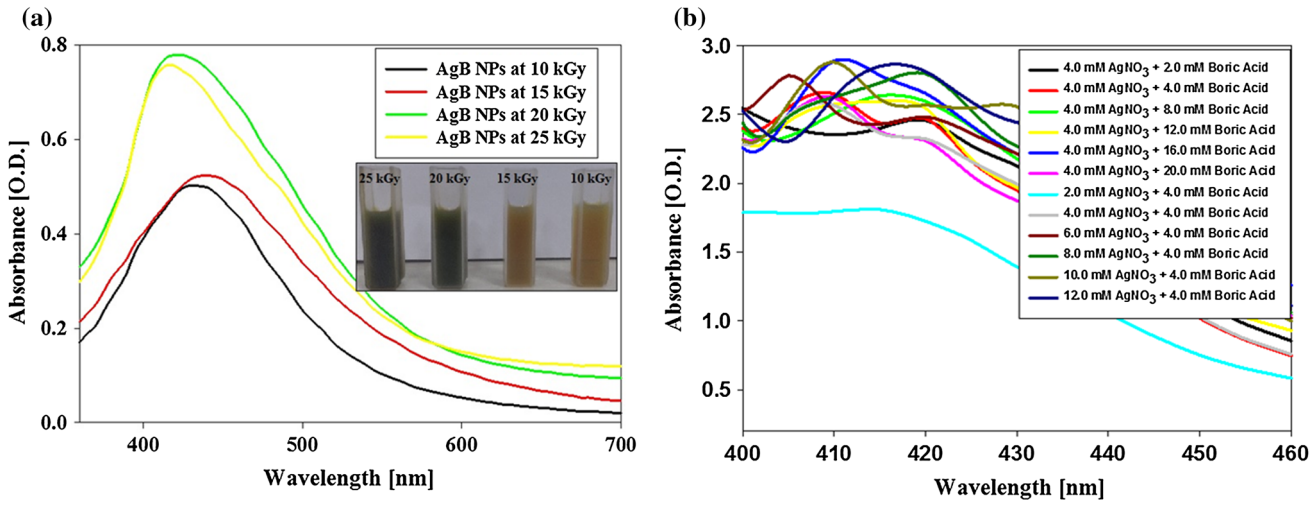

Fig. 3 UV-Vis. spectroscopy of AgB NPs synthesized by PVP and gamma rays where **a** effect of different gamma rays doses (diluted 15 times; Table 2) and **b** optimization of AgB NPs synthesis at different boric acid and silver nitrate concentration (diluted 15 times; Table 3)

Table 2 Maximum absorbance and the corresponding wavelength of AgB NPs synthesized by PVP at different gamma irradiation doses (diluted 15 times)

Different Gamma rays doses (kGy)	Maximum absorbance (O.D.)	Wavelength (nm)
10.0	0.5020	430.0
15.0	0.5230	440.0
20.0	0.7780	420.0
25.0	0.7570	415.0

Table 3 Experimental design for the optimization of AgB NPs production (diluted 15 times)

Run number	Conc. of silver nitrate (mM)	Conc. of boric acid (mM)	Responses: absorbance (O.D.) at λ_{max} range 410.0–420.0 nm
1	4.0	2.0	2.457
2	4.0	4.0	2.649
3	4.0	8.0	2.636
4	4.0	12.0	2.595
5	4.0	16.0	2.890
6	4.0	20.0	2.623
7	2.0	4.0	1.808
8	4.0	4.0	2.566
9	6.0	4.0	2.524
10	8.0	4.0	2.796
11	10.0	4.0	2.800
12	12.0	4.0	2.801

Recommended Reaction Mechanism for Gamma Rays-Promoted AgB NPs Development in the Presence of PVP Polymer

The reduction method explained that AgB NPs synthesis begins following gamma radiation. A reduction is particularly developed only at 20.0 kGy, meaning that radiation possesses an important function in AgB NPs synthesis [11, 22]. Electrons and free radicals which developed in water following gamma rays were e^-_{aq}, H_2O_2, H_2, $OH^{\cdot}$ and $H^{\cdot}$ (Eq. 1). The advantage of gamma radiation for AgB NPs formation was the production of the wanted consequence

of very reducing electron without any harmful byproducts libration [27, 28].

The overall impact considered the application of potential electron as a reducing factor to Ag^+ ions and also PVP as a capping polymer for AgB NPs synthesis. The reaction was starting by the hydrolysis (ionization) of boric acid and silver nitrate to produce their anions and cations such as B $(OH)_4^-$, H^+, Ag^+ and NO_3^- as illustrated in both Eqs. 2 and 3 [11, 44].

Boric acid is identified as a weak Lewis acid. The small acidity of it was generated from the facility to receive OH^-. It hydrolyzed and ionized in the free solution such as water (Eq. 3) provides a perspective concentration of the [B $(OH)_4]^-$ anion [44, 45].

Additionally, the base [B $(OH)_4]^-$ that combined with $B(OH)_3$ were the novel and important boron species in the borate solution [44]. Both [B $(OH)_4]^-$ and $B(OH)_3$ were condensed to produce a complex system and were identified as the poly-borates [44]. The general and significant poly-borate species in the aqueous solutions are named as a tri-borate mono-anion, $[B_3O_3(OH)_4]^-$ [44].

Following that, Ag^+ reduction may be performed by the electron flow from the hydrated electrons to produce Ag NPs (possibility; Eq. 4). The different possibilities can be performed following the ionization of borate, anion [B $(OH)_4]^-$ was conducted with Ag^+ to create the composite NPs (Ag $B(OH)_4$; Eq. 5) [46].

It must be noted that the free radicals $H^\cdot$ and $OH^\cdot$ were ready to separate the hydrogen atom from the PVP producing a PVP radical (developed radicals = $(C_6H_8NO)\ n^\cdot$; Eq. 6). After that, a PVP radical was acted with Ag^+ to produce steady and stabilized Ag NPs and a regular PVP polymer (Eq. 7). Subsequently, the steady PVP can keep Ag NPs and/or Ag $B(OH)_4$ more constant and respond by the association with them (Eq. 8).

$$H_2O \xrightarrow{\gamma-ray(Radiolysis)} e_{aq}^- + OH^\cdot + H^\cdot + H_2 + H_2O_2 \quad (1)$$

$$AgNO_3 + H_2O \xrightarrow{Hydrolysis} Ag^+ + NO_3^- \quad (2)$$

$$B(OH)_3 + 2H_2O \xrightarrow{Hydrolysis} [B(OH)_4]^- + H_3O^+ \quad (3)$$

$$Ag^+ + e_{aq}^- \xrightarrow{Reduction} Ag^\cdot \quad (4)$$

$$[B(OH)_4]^- + Ag^+ \rightarrow AgB(OH)_4 \quad (5)$$

$$(C_6H_9NO)_n + OH^\cdot \rightarrow (C_6H_8NO)_n^\cdot + H_2O \quad (6)$$

$$(C_6H_8NO)_n^\cdot + Ag^+ + H_2O \xrightarrow{Reduction} Ag^\cdot + (C_6H_9NO)_n + H_3O^+ \quad (7)$$

$$(C_6H_9NO)_n + AgB(OH)_4 \xrightarrow{Stabilization\ and\ capping} (C_6H_9NO)_nAgB(OH)_4 \quad (8)$$

Characterization of Silver Boron Nanoparticles

X-ray Diffraction Analysis

XRD shows a crystal composition and the organization of the identified NPs because it provides the crystal size and the position of the observed atoms [9, 47, 48]. XRD investigations were exhibited in Fig. 4a and b.

Figure 4a illustrates the XRD interpretation of the PVP polymer which was presented two identical peaks at 12.28° and 21.74°, which are associated with the amorphous nature of PVP [49]. Also, Fig. 4b represents XRD analysis of the synthesized AgB NPs which have not involved any

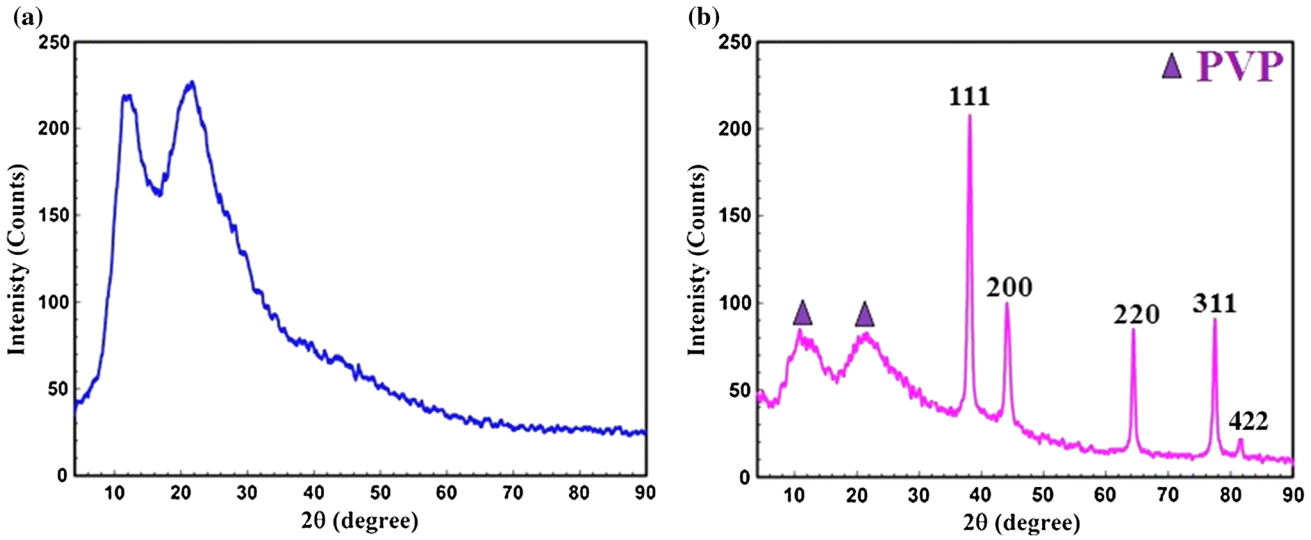

Fig. 4 XRD analysis for **a** non-irradiated PVP and **b** the synthesized AgB NPs by PVP and gamma rays at 20.0 kGy

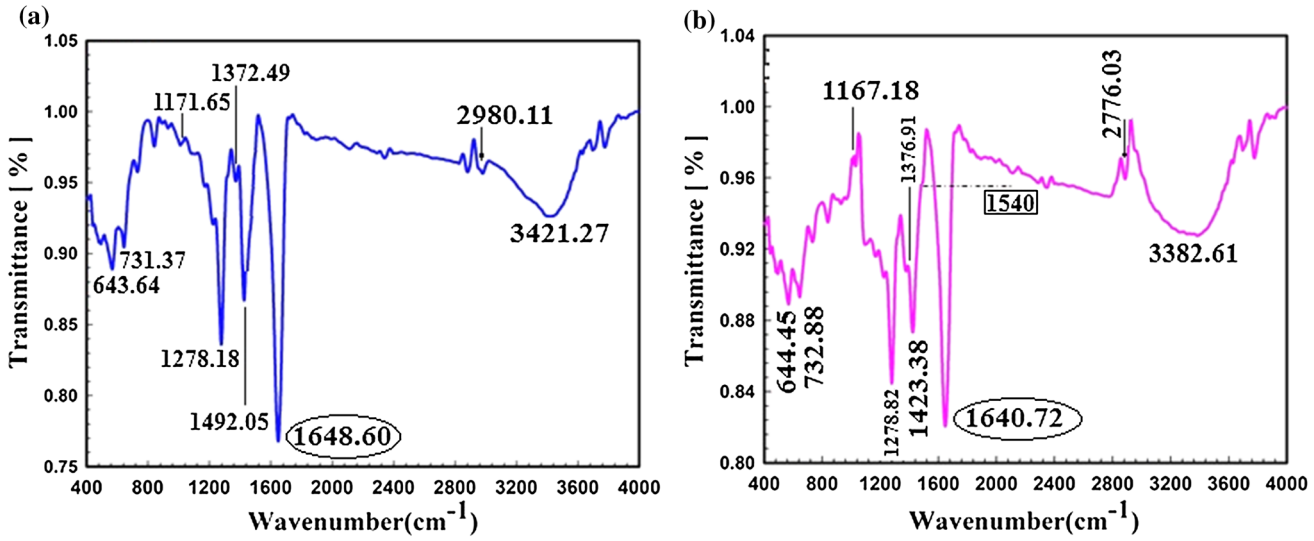

Fig. 5 FTIR spectrum for **a** non-irradiated PVP and **b** the synthesized AgB NPs by PVP and gamma rays at 20.0 kGy

Table 4 FT-IR spectrum of non-irradiated PVP and AgB NPs synthesized by PVP and gamma rays at 20.0 kGy, and its corresponding assignment with literature references

PVP (wave-number cm^{-1})	AgB NPs-PVP (wave-number cm^{-1})	Assignment with the literature references
3421.27	3382.61	Stretching vibrations O–H bond [56, 58, 59]
2980.11	2776.03	CH_2 asymmetric stretching [56, 58, 59, 63]
1648.60	1640.72	Symmetric and asymmetric of C=O [53–59, 63], also the wave number changes may result from bond weakening due to reverse bonding by the incomplete contribution of the lone pair electrons of oxygen in PVP to the empty orbital of silver boron NPs [64]
–	1540.00	Agreeing to N–H bond which created following the ring break because of the entire PVP oxidation through gamma rays and matching with a constant silver ions reduction to produce silver boron NPs, and not observed in real non-irradiated PVP [65]
1492.05	1423.38	Vibration of C=N (pyridine ring) [54, 58, 59], and the drop in the wave number may result from PVP ring crack because of the full oxidation with gamma radiation and corresponding with a constant reduction of silver ions to create silver boron NPs [65]
1372.49	1376.91	C–H bending of CH_2 or OH bending [53, 58, 59, 63].
1278.18	1278.82	CH_2 (wagging or twisting) or N–OH complex [53–55, 58, 60, 63]
1171.65	1167.18	C–C stretching [53, 58, 60, 63]
731.37	732.88	Out-of-plane rings C–H bending/C–N stretching vibration [53, 58, 60, 63]
643.64	644.45	C–N bending [53, 58, 60, 63]

peak regards to the starting ingredient materials (boric acid and/or silver nitrate) but for PVP (Fig. 4a) that included in the construction and capping. The measurement of XRD for each component expresses the growth of the nano-complex.

XRD concerning the synthesized AgB NPs (Fig. 4b) shows the characteristics diffraction highlights with 2θ such as 38.09°, 44.61°, 64.36°, 77.00°, and 81.59° where these peaks describe the Bragg's reflections (111), (200), (220), (311) and (422) respectively (JCPDS card no. 04-0783) [10, 11, 19, 21, 27, 50, 51]. This indicates that the incorporated AgB NPs were crystalline in nature. Its necessity to be noted that there is a little shifting in 2θ which may be because of the construction of AgB NPs [9, 47].

Definitely, there are two amorphous peaks toward 11.70° and 20.26° concerning the PVP polymers (Fig. 4b) that involved in the structure and capping of AgB NPs but the peaks possess the intensity less than that found in the pure PVP. The lack of certain peaks at 31.30°, 32.62° and 33.68° means that the synthesized AgB NPs are pure and freed of silver oxide nanoparticles AgO NPs [52].

Fourier Transform Infrared Analysis

Figure 5 illustrates the FTIR investigation of AgB NPs and PVP. FT-IR spectrum report and its assignments for AgB NPs incorporated PVP and PVP are presented in Table 4 which compared with the literature articles [53–61]. FTIR of the incorporated AgB NPs with PVP (Fig. 5b) revealed that there is incorporation between C=O of the PVP polymer and silver boron complex (AgB $(OH)_4$; Eq. 8). PVP owns C=O and C–N bonds (the functional groups) which control the affinity for silver ions and its complex [62]. It seems that the inclusion of PVP polymers within the metal colloidal system (AgB $(OH)_4$) depends on the size and the concentration of the colloidal NPs [63].

C=O peak (at 1648.60 cm^{-1}) in the non-irradiated PVP (Fig. 5a) was converted to 1640.72 cm^{-1} including a small broadening in the AgB NPs/PVP composite. This turn was agreeable with those reported by Zhang et al. [64]. The reduction in the wave numbers for C=O peak may happen from bond weakening and due to the opposite bonding by the inadequate participation of the lone pair of electrons founded in PVP oxygen to AgB nano-complex (AgB $(OH)_4$) and approved the incorporation of AgB NPs with PVP C=O functional group [64].

It must noted that, the peak at 1492.05 cm^{-1} was agreeing to the C=N vibration (established in the pyridine ring), and the decrease in the wave number in AgB NPs/PVP FTIR spectrum (1423.38 cm^{-1}), also, the appearance of new N–H (1540.0 cm^{-1}) may happen from the ring fracture regarding the complete oxidation of PVP by 20.0 kGy gamma rays [65] which may be matching with the constant reduction of silver ions to form AgB NPs (Eqs. 4 and 5).

High Resolution Transmission Electron Microscopy (HRTEM), and Dynamic Light Scattering (DLS)

To examine the average particle size and the shape of the synthesized AgB NPs, TEM images were conducted, and its outcomes were associated with the DLS examination [27, 66]. HRTEM image described the different shapes of the synthesized AgB NPs like an oval and spherical in a scale ranging from 19.90 nm to 35.80 nm with the mean average diameter around 29.55 nm as shown in Fig. 6a. The common particle size distribution was determined by DLS method and was defined as 71.21 nm in the AgB NPs incorporated by PVP and gamma radiated at 20.0 kGy as illustrated in Fig. 6b.

It was suggested that DLS size of AgB NPs (71.21 nm) was noted to be greater than HRTEM size (29.55 nm). The answer because of DLS investigates the hydrodynamic width where the synthesized AgB NPs were enclosed by the water molecules and may the reason for the great size of the capped NPs [10, 27, 67, 68].

Scanning Electron Microscopy (SEM) and Energy Dispersive of X-Ray (EDX) Spectroscopy

The uniform display of the synthesized AgB NPs and the surface morphology are presented in Fig. 7a. It can be noticed that Ag and B NPs were separated exactly in the adjusted nano-composite which shows as a bright particle. PVP polymers are used in AgB NPs construction and

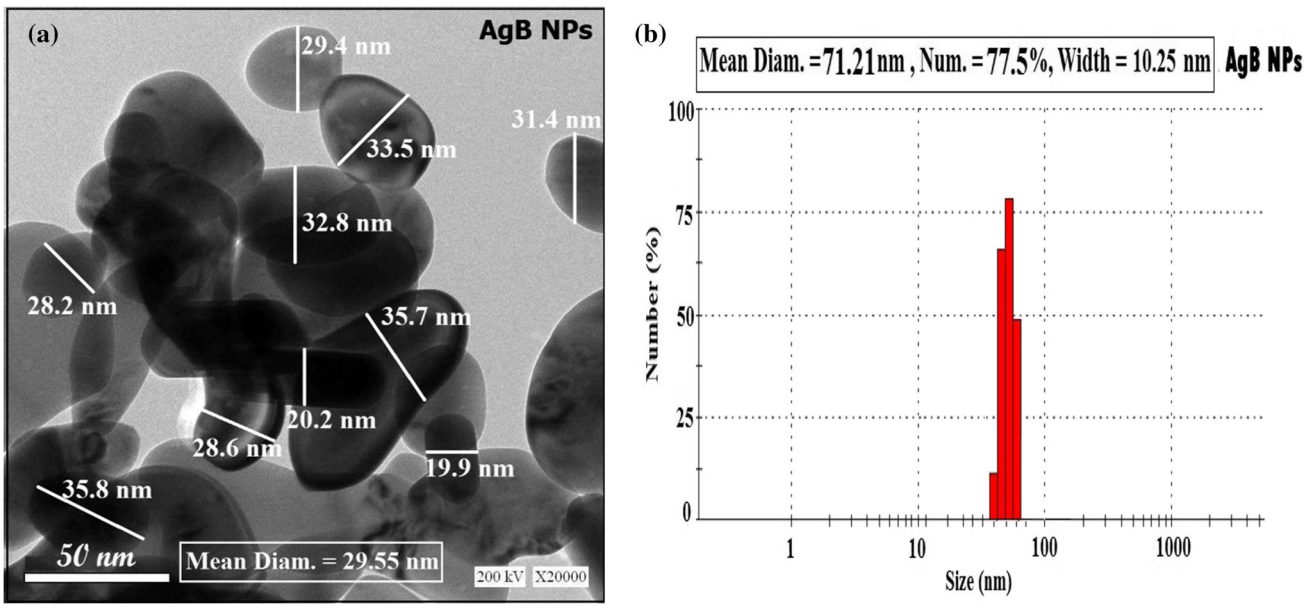

Fig. 6 Shape and size distribution of the synthesized AgB NPs by PVP and gamma rays at 20.0 kGy where **a** HRTEM image and **b** DLS analysis

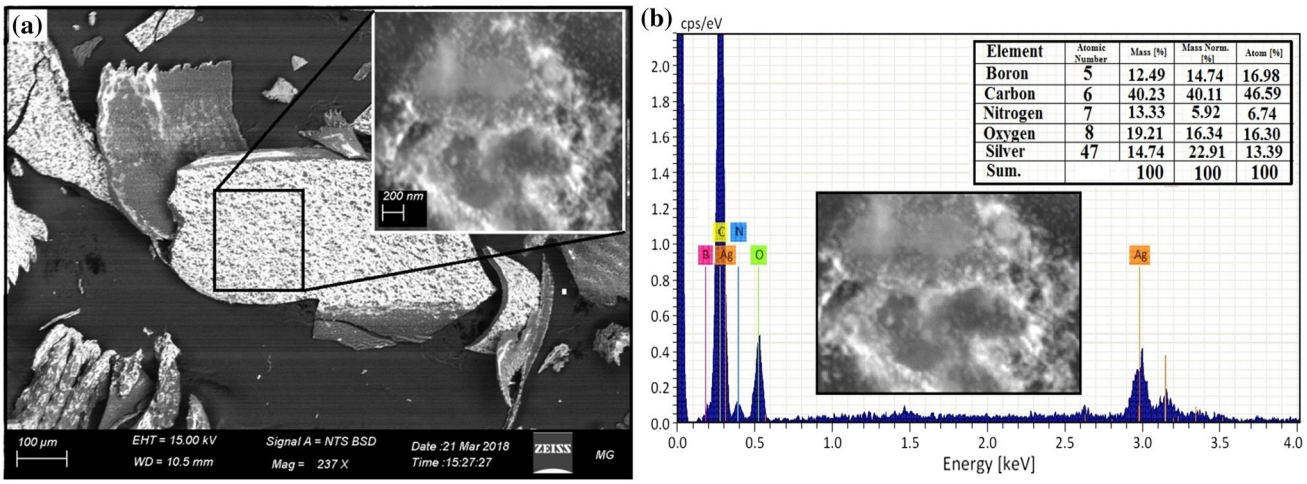

Fig. 7 Morphological characters, purity and elemental analysis of the synthesized AgB NPs by PVP and gamma rays at 20.0 kGy where **a** SEM image of the homogenous nano-composite (Ag & B NPs) distribution, and **b** the corresponding EDX elemental analysis

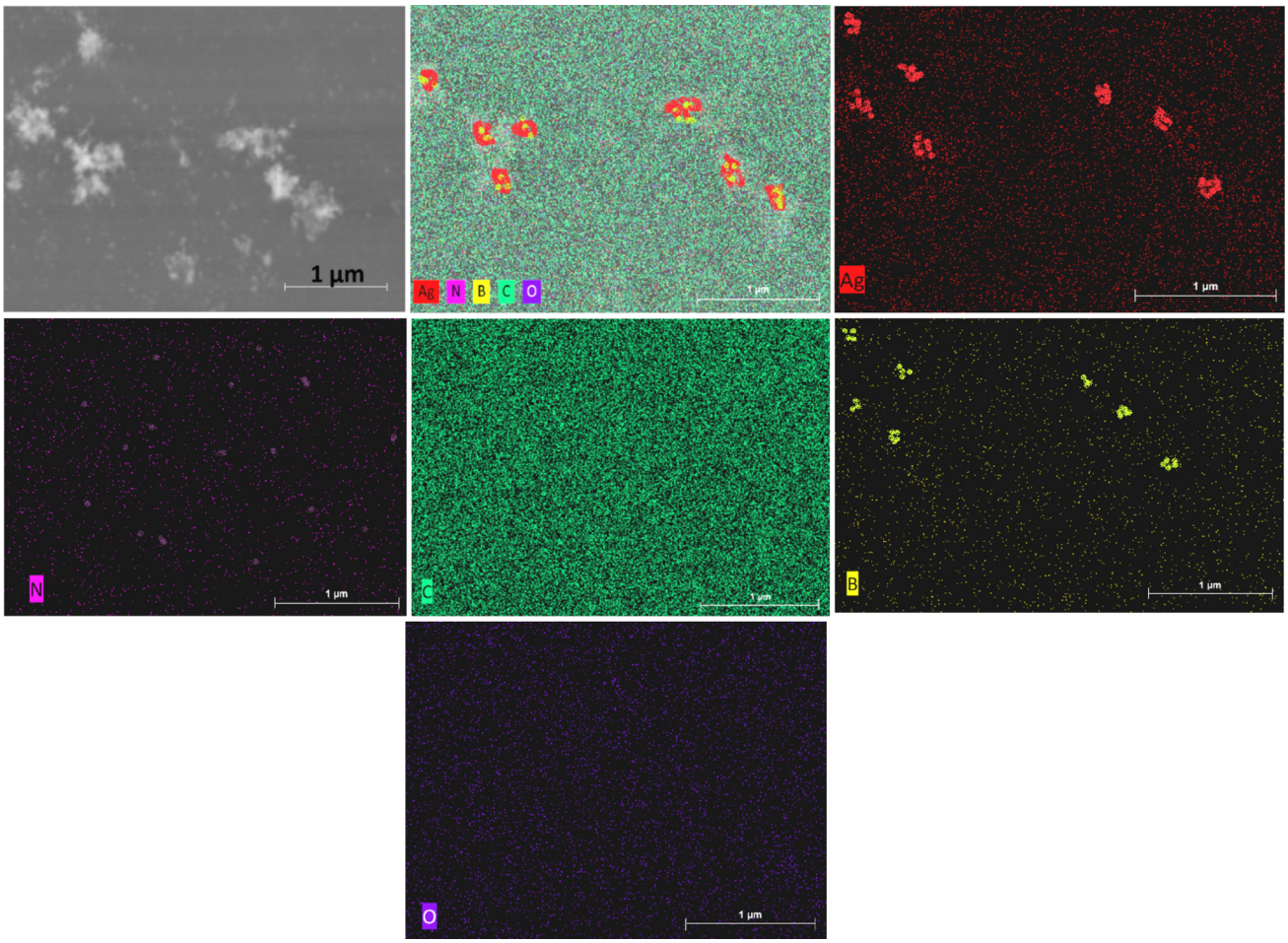

Fig. 8 SEM/EDX mapping images of the synthesized AgB NPs by PVP and gamma rays at 20.0 kGy

Table 5 Impact of the tested treatments, their concentrations and period of application on *M. incognita* juvenile's mortality (In vitro)

Treatments	Conc.	Incubation periods											
		24 h			48 h			72 h			96 h		
		Dead juveniles	A live juveniles	Mortality (%)	Dead juveniles	A live juveniles	Mortality (%)	Dead juveniles	A live juveniles	Mortality (%)	Dead juveniles	A live juveniles	Mortality (%)
1	100%	2.66^{efg}	16.33	14.01	3.33^{fg}	15.66	17.53	3.66^{hij}	14.66	19.97	4.00^{efg}	15.33	21.05
	50%	2.00^{gh}	17.33	10.34	2.66^{gh}	16.66	13.76	3.33^{ijk}	16.00	17.22	3.00^{gh}	15.66	16.07
	25%	1.66^{gh}	17.66	8.59	2.00^{hi}	17.33	10.34	2.66^{kl}	16.66	13.76	3.00^{gh}	16.66	15.25
2	100%	5.00^{c}	13.66	26.79	5.33^{c}	13.66	28.06	6.33^{d}	12.00	34.53	6.66^{c}	13.66	32.77
	50%	3.33^{def}	14.66	18.51	4.66^{cd}	15.33	23.31	5.00^{ef}	14.66	25.43	5.66^{cd}	14.66	27.85
	25%	2.66^{efg}	16.33	17.01	3.66^{ef}	15.33	19.27	4.33^{fgh}	15.66	21.66	4.66^{def}	14.33	24.53
3	100%	10.66^{a}	8.66	55.17	11.66^{a}	9.00	56.43	12.66^{a}	6.33	66.66	15.33^{a}	5.33	74.20
	50%	6.66^{b}	12.331	35.07	8.33^{b}	10.66	43.86	9.33^{c}	9.66	49.13	12.66^{b}	7.00	64.39
	25%	4.33^{cd}	14.66	22.80	4.66^{cd}	14.66	24.12	5.33^{e}	14.33	27.11	6.33^{c}	12.66	33.33
4	100%	11.00^{a}	8.33	56.91	12.33^{a}	10.00	55.21	13.33^{a}	7.66	63.51	14.66^{a}	5.66	72.14
	50%	7.66^{b}	13.00	37.07	8.66^{b}	11.00	44.04	10.33^{b}	8.66	54.39	11.66^{b}	7.66	60.35
	25%	3.66^{de}	15.33	19.27	4.66^{cd}	16.33	22.20	5.33^{e}	15.66	25.39	6.3^{c}	16.66	27.43
5	100%	3.66^{de}	15.66	18.94	4.33^{de}	14.33	23.20	4.66^{efg}	13.66	25.43	5.00^{de}	13.33	27.27
	50%	2.66^{efg}	16.66	13.76	4.00^{def}	15.33	20.69	4.00^{ghi}	15.00	21.05	3.66^{fgh}	14.33	20.34
	25%	2.33^{fgh}	17.33	11.85	2.66^{gh}	16.33	14.01	3.00^{jkl}	15.66	16.07	3.33^{gh}	14.66	18.51
Control		1.30^{h}	18.33	6.62	1.66^{i}	17.33	8.74	3.00^{l}	17.00	15.00	2.66^{h}	17.33	13.30
LSD 5%		1.046			0.989			0.865			1.018		

Means in each column followed by the same letter (s) are not significantly different at 5% level, Data within the groups are analyzed using one-way analysis of variance (ANOVA) followed by $^{a, b, c, d, e, f, g, h, i, j, k, l}$ Duncan's multiple range test (DMRT)

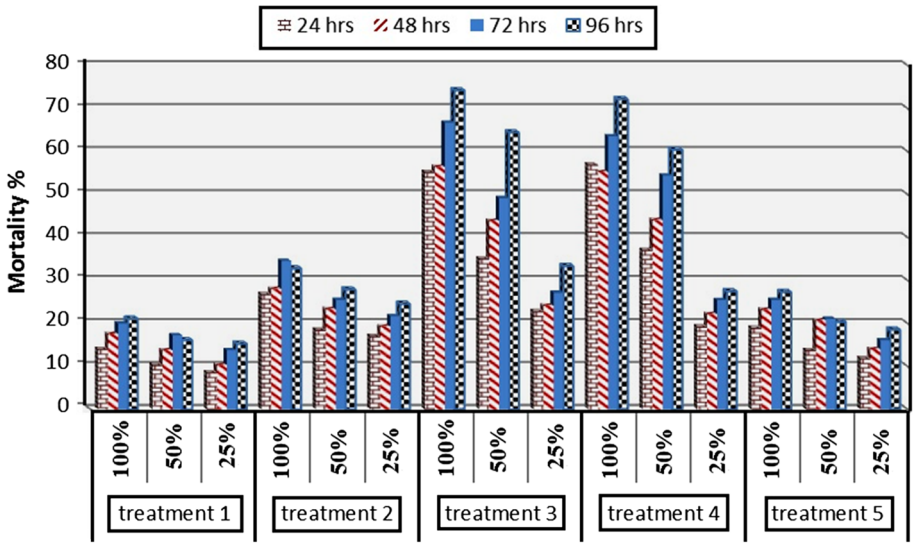

Fig. 9 Impact of the tested treatments (Table 1), their concentrations and period of application on the 2nd juvenile's mortality (in vitro study)

capping which appears to include with the synthesized AgB NPs.

EDX elemental method is an analytic technique applied for the elemental study or chemical characterization of the fabricated samples [9, 10, 23, 47, 48]. The EDX investigation confirm that the synthesized AgB NPs (Fig. 7b) is stoichiometric and similar with a formal arrangement. The characteristic X-ray peaks of Ag, O, N, C and B atoms are evident in EDX of AgB NPs, additionally, O, N and C atoms are corresponding to the PVP polymer.

SEM/EDX Mapping Images of the Synthesized AgB NPs

The elemental mapping images of the synthesized AgB NPs are represented in Fig. 8. The images are classified as Ag, B, N, O, and C for AgB NPs. From these colored figures, it is clear that AgB NPs are comparable in terms of the features of Ag, and B atoms at the same position (red for Ag and yellow for B). Also, N, O, and C were atoms related to the structure of the PVP polymer.

Impact of the Examined AgB NPs Treatments, Their Concentrations and Duration of the Their Application on *M. incognita* Juveniles Mortality (In Vitro)

Root-knot nematodes are dangerous pathogens that produce critical destruction to the major crops [69]. The results represented from Table 5 and Fig. 9 exhibited that the treatment 3 showed the greatest percentages of mortality in *M. incognita* 2nd juveniles at all concentrations and the periods of the processing relating to the support of the other treatments. The concentrations at 100, 50 and 25% (treatment 3) were reported 55.17, 35.07 and 22.8% mortality, respectively in the 2nd stage juveniles, following 24 h of the treatment. These percentages of mortality were improved with rising the period of the operation which extended the maximum mortality (74.2, 64.39 and 33.3% for 100, 50, 25%, respectively) following 96 h of in vitro treatment.

It must be regarded that, the results which obtained by application of the treatment 4 were quite similar to those of the treatment 3, where concentrations 100, 50 and 25% of treatment 4 reported 56.91, 37.07 and 19.27% mortality, respectively in the 2nd stage juveniles, following 24 h of the treatment. Furthermore, these mortality percentages were improved with extending the period of processing which gave the maximum mortality of 72.14, 60.35 and 27.43% for 100, 50, 25%, respectively next 96 h.

The considerably opposite were shown in treatment 1 which was reported the lowering mortality percentages of *M. incognita* 2nd juveniles at all concentrations and times, where the concentrations 100, 50 and 25% of treatment 1 were reported 14.01, 10.34 and 8.59% mortality, respectively in the 2nd stage juveniles subsequent 24 h of the treatment. Also, these mortality percentages were developed with extending the period of the treatment which arrived the maximum mortality of 21.05, 16.07 and 15.25% for 100, 50 and 25%, respectively next 96 h.

It must be mentioned that the concentration of Ag in AgB NPs (Table 1) applied in our study to assess the nematicidal properties did not pass the allowable boundary of the elemental silver (< 0.025 mM; 2.5 µg/mL) in the drinking water during short-term individual consumption for 1–9 days through the United States Environmental Protection Agency [1, 70, 71].

Table 6 Impact of the tested treatments and time of application on galls and egg-masses of *M. incognita* infecting tomato plants under greenhouse conditions

Material		Average number of galls/1(g) of root	Reduction (%)	Average number of egg masses/ 1(g) of root	Reduction (%)
Time of application	Treatments				
One week before infection	1	39.00^{ghi}	79.44	16.33^{f}	74.74
	2	27.00^{jkl}	85.76	7.00^{hi}	89.17
	3	20.33^{l}	89.28	2.33^{jk}	96.4
	4	23.33^{kl}	87.7	5.00^{ij}	92.27
	5	32.66^{hijk}	82.78	11.33^{g}	82.48
At the same time of infection	1	61.00^{d}	67.84	39.33^{c}	39.17
	2	42.33^{fgh}	77.68	24.33^{e}	62.37
	3	31.00^{ijkl}	83.65	8.33^{gh}	87.12
	4	35.00^{hij}	81.55	16.33^{f}	74.74
	5	52.33^{def}	72.41	31.66^{d}	51.04
One week after infection	1	103.33^{b}	45.52	47.66^{b}	26.29
	2	56.33^{de}	70.3	31.00^{d}	52.06
	3	41.66^{fghi}	78.03	17.00^{f}	73.71
	4	48.00^{efg}	74.69	21.66^{e}	66.5
	5	80.00^{c}	57.82	41.33^{c}	36.08
Nematode only		189.66^{a}	–	64.66^{a}	–
LSD 5%		10.813		3.244	

Means in each column followed by the same letter (s) are not significantly different at 5% level, Data within the groups are analyzed using one-way analysis of variance (ANOVA) followed by $^{a, b, c, d, e, f, g, h, i, j, k, l}$ Duncan's multiple range test (DMRT

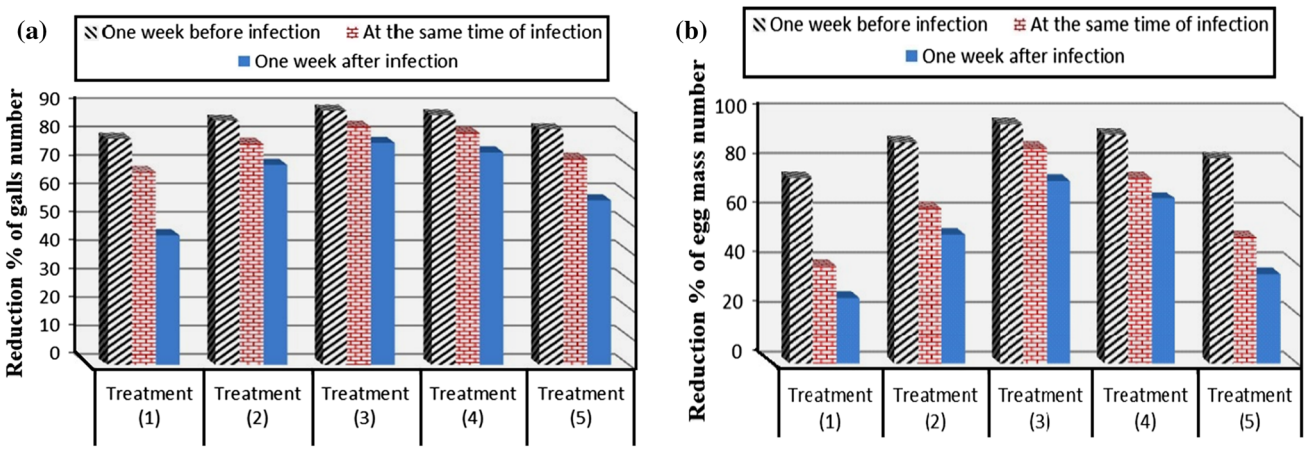

Fig. 10 Impact of the tested treatments (Table 1) and time of application on **a** root galls reduction percentage and **b** egg masses reduction percentage

Effect of the Examined AgB NPs Treatments and Duration of the Their Application on Galls and Egg Mass Numbers in the Infested Tomato Plants with *M. incognita* Under Greenhouse Conditions (In Vivo)

Ag NPs doping with other metals was induced changes in the structural, dielectric and optical properties [18], and also increasing the catalytic activity. The results collected from Table 6 and Fig. 10a and b, showed that the treating of the infected tomato plants with the tested elicitors significantly reduced galls number and egg masses number of nematodes. These responses were changed according to the kind of applied elicitor and further to the periods of the treatment.

Table 7 Impact of the tested treatments and time of application on juveniles, female and developmental stages of *M. incognita* infecting tomato plants under greenhouse conditions

Material		Second stage juveniles/250 g soil		Females/1 g root		Developmental stages/1 g root	
Time of application	Treatments	Average number	Reduction (%)	Average number	Reduction (%)	Average number	Reduction (%)
One week before infection	1	235.00^{d}	43.05	31.00^{hi}	71.47	22.00^{d}	69.58
	2	158.66^{g}	61.55	16.66^{k}	84.67	17.33^{ef}	76.04
	3	111.66^{h}	72.94	6.00^{l}	94.48	5.33^{i}	92.63
	4	87.66^{i}	78.76	10.00^{l}	90.8	8.33^{hi}	88.48
	5	208.33^{e}	49.52	22.33^{j}	79.45	14.66^{fg}	79.73
At the same time of infection	1	323.33^{b}	21.65	52.66^{d}	51.54	28.33^{c}	60.83
	2	200.00^{ef}	51.53	32.66^{h}	69.94	22.66^{d}	68.67
	3	165.00^{g}	60.02	19.66^{jk}	81.91	8.00^{hi}	88.94
	4	250.00^{d}	39.42	27.00^{i}	75.15	6.00^{i}	91.7
	5	280.00^{c}	32.15	43.33^{f}	60.12	30.66^{c}	57.61
One week after infection	1	286.00^{c}	30.69	83.00^{b}	23.61	45.00^{b}	37.79
	2	269.00^{c}	34.81	47.66^{e}	56.14	21.66^{de}	70.05
	3	213.00^{e}	48.38	31.66^{h}	70.86	8.33^{hi}	88.48
	4	185.00^{f}	55.17	39.00^{g}	64.11	11.00^{gh}	84.79
	5	240.00^{d}	41.84	57.33^{c}	47.24	29.00^{c}	59.91
Nematode only		412.66^{a}	–	108.66^{a}	–	72.33^{a}	–
LSD 5%		18.292		4.111		4.664	

Means in each column followed by the same letter (s) are not significantly different at 5% level, Data within the groups are analyzed using one-way analysis of variance (ANOVA) followed by $^{a, b, c, d, e, f, g, h, i, j, k, l}$ Duncan's multiple range test (DMRT)

The most efficient and active elicitor in decreasing root galls and egg masses numbers in the infected tomato plants through 1 week following infection was treatment 3 that showed 20.33 galls and 2.33 egg masses with a reduction percentage of 89.28 and 96.4%, respectively. It was subsequently by treatment 4 which registered 23.33 galls and 5.0 egg masses with a reduction percentage of 87.7 and 92.27%, respectively.

It was observed that by applying the treatment 1 during 1 week before the infection, it was reported 39.0 galls and 16.33 egg masses with a reduction percentage of 79.44 and 74.74%, respectively.

In the existing study, the stimulations of the systemic resistance of tomato seedlings toward root-knot nematode by the synthesized AgB NPs and the concerned mechanisms were examined. According to the existing results, the synthesized AgB NPs were strong inducer in the stimulation of the resistance of the disease. Actually, all AgB NPs treatments have significantly generated a reduction in all nematode parameters. This analysis proved that AgB NPs have efficacy to decrease the nematode infestation through the pretreatment of the plant seedlings with AgB NPs.

Effect of the Examined AgB NPs Treatments and Duration of the Their Application on the 2nd Stage Juveniles, Females and Developmental Stages in the Infested Tomato with *M. incognita* Under Greenhouse Conditions (In Vivo)

The results collected from Table 7 and Fig. 11a–c indicated that the treating of the infected tomato plants with the established elicitors significantly reduced the numbers of the 2nd stage juveniles/250 gm soil, females and developmental stages/1 gm root. These responses were modified according to the character of the adopted elicitor and the course of the treatment.

The most potent and effective elicitors in reducing the numbers of the second stage juveniles/250 gm soil in the infected tomato plants were treatment (4 and 3) at 1 week after the infection which recording the reduction percentage of 78.6 and 72.94%, respectively.

The most influential and powerful elicitors in decreasing the numbers of females/1 g root were a treatment 3 and 4 following 1 week and before the infection which reporting a reduction percentage of 94.48 and 90.8%, respectively.

As concerns to developmental stages the most efficient and active elicitor in diminishing their numbers/1 g root

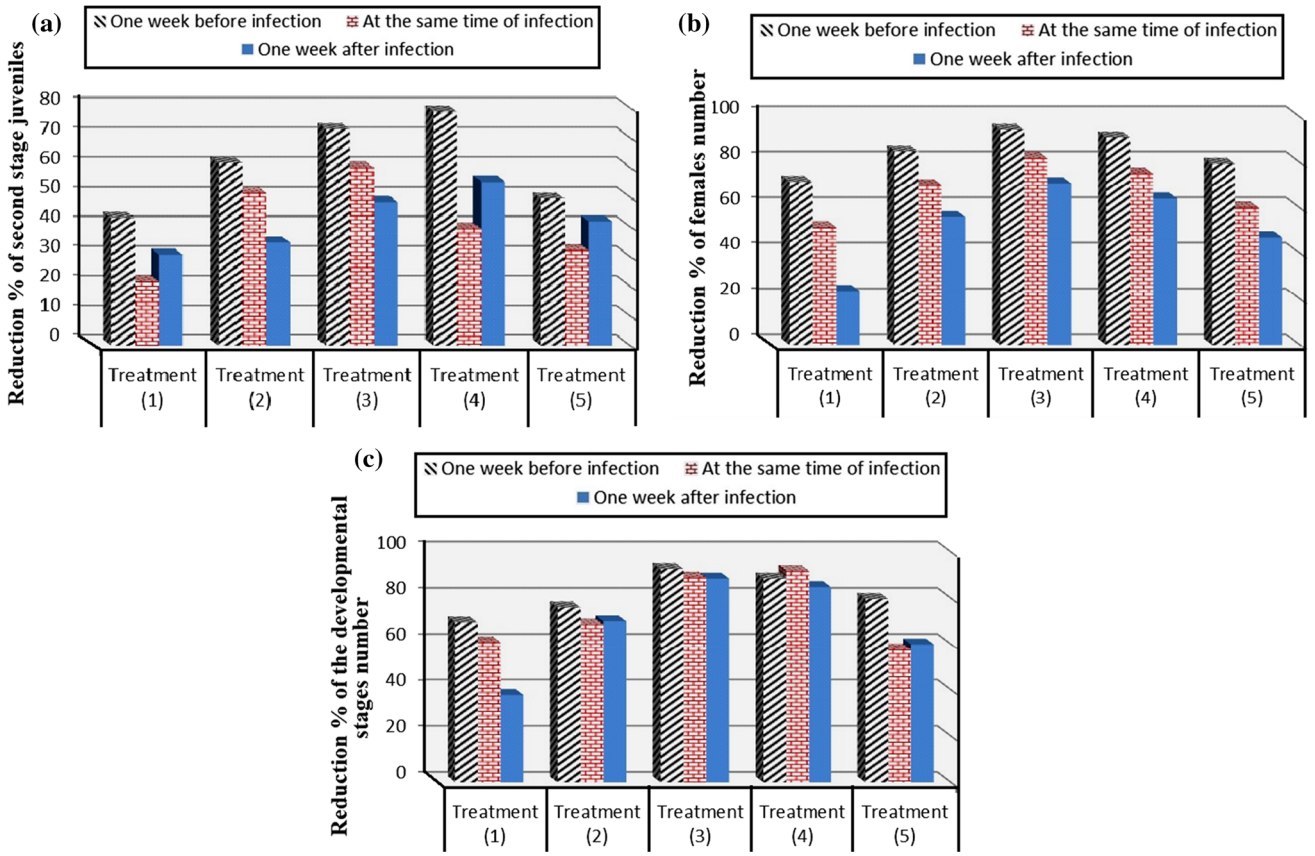

Fig. 11 Impact of the tested treatments (Table 1) and time of application on **a** second stage juveniles reduction percentage **b** females reduction percentage and **c** developmental stages reduction percentage

was the treatment 3 following 1 week and before the infection which showed 5.33 with a reduction percentage of 92.63%.

It must be remarked that at the corresponding time of the infection with nematode both treatments 4 and 3 (Table 1) presented the identical average number about 6.0 and 8.0 with a reduction percentage of 91.7 and 88.94%, respectively. They were followed by the treatment 3 (at 1 week following infection) which provided a great reduction percentage in the developmental stages/1 g root ended 88.48% with a common number as 8.33. The synthesized AgB NPs (treatment 3 and/or 4; Tables 1, 5, 6 and 7) occupy nematicidal action that may present an alternative to high-risk artificial nematicides or irregular biological control factors.

No procedures are now possible to effectively preserve crops toward the parasitic nematodes. The purposes of this research were the initiation of the systemic immunity in the tomato crops upon root-knot nematode (*M. incognita*) disease. The induction of its protection by several NPs elicitors recognized as a novel effective process that becomes generally accepted for managing the plant nematodes, as a plan to reduce the range of environmental depravity and the impact of the unnecessary deadly nematicides.

In over all, the collected results exhibited that both treatment 3 and 4 were the most useful treatments which reported the largest percentages of mortality in *M. incognita* 2nd juveniles at all concentrations comparing to the other treatments.

This study contributed a record that the synthesized AgB NPs possess the capacity for control of root-knot nematodes and these results were matched with Cromwell et al. [32]. Inactivation of *M. incognita* by immediate treatment and decrease of it in the treated soil proved the great nematicidal results of the synthesized AgB NPs (treatments 3 & 4; Table 1).

Additionally, the nematicidal impact of the synthesized AgB NPs toward root-knot nematodes is not the equivalent. Furthermore, particularly the elevated boron concentrations (treatment 3 and 4) are poisonous to the nematode and the various practical treatments in the mortality of *M. incognita* 2nd juveniles were at all concentrations and the duration of the treatments.

The nematode development cycle begins by the eggs, which are detected in the soil and in the crops tissues. The

2nd stages juveniles produce from the eggs were hunting the plant hosts and spoil the root near to its tip. Inside the root, the 2nd stage juvenile's root-knot nematodes found a feeding situation and cause the development of the giant cells. The present nematodes convert to the sedentary and molt four times to stand development. The adult female inserts its eggs in a viscous mass. After that, they can be readily identified by the galls or knots since they eating and easily developed [72].

No surprise that the maximum protection is recorded for Ag NPs in the infection control and the disease treatment within the agriculture area. This universality of the synthesized Ag NPs has created anxiety regarding arranging and distributing Ag NPs as a pesticide [73].

The action mechanism of the synthesized AgB NPs being the anti-nematode tool is expected to include obstructing various cellular mechanisms like membrane permeability, ATP organization, and response to the oxidative tension in the nematode cells [74].

On the other hand, Ag NPs in the synthesized AgB NPs are a broad-spectrum antimicrobial agent which able to damage the pathogenic bacteria and fungi which invading the plant [75, 76]. It is likely that, Ag NP holds an antifungal impact on many root-connected fungal microbes (like *Rhizoctonia solani* and *Gaeumannomyces graminis*) which treated with it and may display further tolerant to the nematode injury due to remarkable stability from further pressure by the other pathogens. Additionally, there are several detailed studies [45, 46, 77, 78], concerning the antimicrobial action of boron which doped with various elements to produce boron nano-composites.

Investigations confirm that sufficient boron diet enhances root absorption of potassium and phosphorus through supporting own capacity (by ATPase potential) and of root cell layers composition [34]. Boron owns an essential part in the founding of the roots by mycorrhizal molds, which provides to root absorption of the phosphorus [38]. In amazing tests with maize seedlings, the decreased root absorption of the potassium and phosphorus following low boron quantity was returned in 1 h following boron addition to the developing medium [35]. Laboratory data further recommends that a sufficient boron amount is required for the reduction of aluminum poisoning in the seedlings which planted in a low pH clays [79].

Boron NPs incorporated with Ag NPs ultimately discharged from the synthesized nano-composite inside the tomato plant tissue so boron was concerned as nano-nutrient which diffused quickly into the plant cell membrane without obtaining a boron-polyol network [33].

Boron incorporated with Ag NPs owned imported impact toward the growth parameters such as plant length, the chlorophyll content, leaf quantities, whole biomass, dry matter addition, increased weight and tuber production [34]. Beside the characteristic parameters such as water soluble and/or reducing carbohydrate decreasing, the improvement in starch and tuber ash rate, good fertilizer in the nano-scales and finally developing the plant resistance toward any soil infected pathogens [3, 33–35, 38].

Boron NPs, when involved in a little amount, may serve as bio-stimulators which are elements other than soil improvers, fertilizers or pesticides that affected the plant metabolic improvements like the plant respiration, cell division, ions absorption and photosynthesis [80].

The utilization of the synthesized AgB NPs at the three time of infection (Tables 6 and 7) enhances the physiological resistance of the tomato plant. Owing to the antimicrobial and the hormone like properties of the synthesized AgB NPs, they may be developed the whole protein concentration in crops [81, 82]. Additionally, they were influencing the plant's individual protection mechanisms by the previous treatment of the inducer (AgB NPs) that may be a unique tomato plant strength plan [83].

Additionally, based on the modern understanding of the biochemistry of physiological resistance of the tomato plant, it can be assumed that the systemic immunity may be effected from the creation of various parameters such as the differences in the cell wall structure and the construction of phytoalexins and pathogenesis associated proteins [84]. Further, the organization of phytoalexins is usually linked to the caused resistance steps of the synthesized AgB NPs [84].

Some plants generate a wide mixture of the secondary outcomes that include phenol and different group as a reply behind several NPs operation. They could be an essential portion of the plant's protection system toward insects and infections like root-knot nematodes [85]. Some phenols are considered as pre-infection inhibitors, giving the crop with a specific level of primary defense toward pathogenic bacteria, fungi and pests [86].

Furthermore, there are amazing examples showing that the activation of polyphenol oxidase (PPO) and peroxidase (POD) performs a significant purpose in the natural switch and protection of the tomato plant from the pathogenic invasion. It was stated that POD may be remarkable ingredients in the support methods that are excited in the tomato crops in reply to pathogen disease [87].

It must be mentioning that the acute toxicity of boron nanoparticles (B NPs) was estimated by Strigul et al., [88], and was found that, B NPs with EC_{50} ranging from 56.0 to 66.0 mg/L, depending upon the age of the solution and can be classified as harmful to aquatic environment when EC_{50} was at 100 mg/L.

Additionally in our research the concentration of B NPs in the most effective treatment 3.0 (Table 1) was found to be 43.03 mg/L, so the tested B NPs in the synthesized AgB NPs was safe to use in the nematode treatment.

Finally, it's known that less than 43.03 mg/L of B NPs (due to the tomato plant uptake) may be introduced and released in the aqueous solution, so it will not cause health risk to the environment.

By making a comparative study between the nanomaterial-based nematode treatment [1, 3, 7, 8, 32] and the synthesized AgB NPs we found that, the treatment was conducted by utilizing only one kind of nanoparticles without taking into consideration the toxicity of the treatment.

There are a lot of researches deals with the treatment by Ag NPs only, Kalaiselvi et al., [1] synthesized a biogenic Ag NPs and investigate the management of root-knot nematode after the treatment with various concentrations (100, 250, 500 and 1000 ng/mL) of Ag NPs synthesized by *Euphorbia tirucalli.* Another study performed by Abbassy et al., [3], regarding the treatment of root-knot nematode by the synthesized Ag NPs at different concentration 125, 250, 500 and 1000 μg/mL.

In order to inhibit the embryonic development, hatching and reproduction of *Meloidogyne incognita* Couto et al., [36], estimated the activity of boron at different concentrations and results indicated that boron controlled nematode population at the dose of 400 g/L (stock solution) and promoted juvenile hatching when used at maximum dosage on the eighth day.

In our research we choose the silver and boron nanocomposite for nematode treatment by utilizing an eco-friendly and cost-effective method to make an encourage benefits between both of them and decreasing the toxicity to aquatic environment after the conjugation. It was found that the concentration of Ag NPs was 10.0 mg/L and 43.03 mg/L for B NPs in the treatment 3.

Positively, the conclusion from this study symbolized that AgB NPs obtained a high action toward the root-knot nematode in vitro as well as in vivo. Accordingly, the decision indicate that it must be applying nanotechnology as a protection technique for the individual and the environment to control the root-knot nematode.

Finally to get a further definite sign on the induced systemic resistance (ISR), some of the signal elements and sign transductions like phenolic mixtures, antioxidant enzyme actions, the endogenous hormonal content particularly (salicylic, jasmonic, and abscisic acids), of the examined plants must be determined in our future work.

Conclusion

In our opinion, this research suggests a new cost-effective and eco-friendly synthesis of AgB NPs using PVP polymer and gamma rays for nematode treatments. The complete characterization were conducted to determine the morphology, crystallinity, purity, distribution and the average particle size of the synthesized AgB NPs, which confirmed to be rounded and/or oval with an average size of 29.55 nm. A suggested reaction mechanism describes the potential and constant reduction of silver and boron ions following the oxidation of PVP by 20.0 kGy gamma rays. FTIR analysis confirms the ring opening of PVP which encourage the oxidation of polymer. The synthesized AgB NPs were a promising agent which inhibit the invasion of root-knot nematode that infected the tomato seedlings. They were decreased the numbers of root galls, egg masses, the 2nd stage juveniles, females and developmental stages following 96 h of the treatment. In treatment 3, the mortality% were developed with extending the time of the treatment which ended the maximum mortality of 74.20, 64.39 and 33.30% for 100, 50 and 25%, respectively after 96 h. Additionally, the concentration of Ag NPs was 10.0 mg/L and 43.03 mg/L for B NPs which give a great activity at low concentrations. After our research finding, the synthesized AgB NPs were a promising composite in the agricultural, nanoparticles-based soil control, food processing and as a new effective technique for controlling the root-knot caused by *Meloidogyne incognita*.

Acknowledgements The authors would like to thank the Nanotechnology Research Unit (P.I. Prof. Dr. Ahmed I. El-Batal), Drug Microbiology Lab., Drug Radiation Research Department, NCRRT, Egypt, for financing and supporting this study under the project "Nutraceuticals and Functional Foods Production by using Nano/Biotechnological and Irradiation Processes". Also, the authors would like to thank Prof. Mohamed Gobara (Professor at Military Technical College), Dr. Mohamed M. Ghobashy (Associate Professor at NCRRT), Dr. Muhammad I. Abdel Maksoud (Lecturer at NCRRT), and Zeiss microscope team in Cairo for their invaluable advice during this study.

Compliance with Ethical Standards

Conflict of interest The authors declare that they have no conflict of interest.

Research Involving Human Participation and/or Animals This article does not contain any studies with human and/or animals performed by any of the authors.

Informed Consent Not applicable.

Ethical Approval Not applicable.

References

1. D. Kalaiselvi, A. Mohankumar, G. Shanmugam, S. Nivitha, and P. Sundararaj (2019). *Crop Prot.* **117**, 108–114.
2. D. M. Bird and I. Kaloshian (2003). *Physiol. Mol. Plant Pathol.* **62**, (2), 115–123.

3. M. A. Abbassy, M. A. Abdel-Rasoul, A. M. Nassar, and B. S. Soliman (2017). *Arch. Phytopathol. Plant Prot.* **50**, (17–18), 909–926.
4. M. Hussain, T. Mukhtar, and M. Kayani (2011). *J. Anim. Plant Sci.* **21**, (857), 861.
5. H. Regaieg, M. Bouajila, L. Hajji, A. Larayadh, N. Chiheni, I. Guessmi-Mzoughi, and N. Horrigue-Raouani (2017). *Arch. Phytopathol. Plant Prot.* **50**, (17–18), 839–849.
6. S. B. Milligan, J. Bodeau, J. Yaghoobi, I. Kaloshian, P. Zabel, and V. M. Williamson (1998). *Plant Cell* **10**, (8), 1307–1319.
7. A. H. N. El-Deen and B. A. El-Deeb (2018). *J. Agric. Sci.* **10**, (2), 148.
8. A. M. Nassar (2016). *Asian J. Nematol.* **5**, (1), 14–19.
9. M. A. Maksoud, G. S. El-Sayyad, A. Ashour, A. I. El-Batal, M. S. Abd-Elmonem, H. A. Hendawy, E. Abdel-Khalek, S. Labib, E. Abdeltwab, and M. El-Okr (2018). *Mater. Sci. Eng., C* **92**, 644–656.
10. A. Baraka, S. Dickson, M. Gobara, G. S. El-Sayyad, M. Zorainy, M. I. Awaad, H. Hatem, M. M. Kotb, and A. Tawfic (2017). *Chem. Pap.* **71**, (11), 2271–2281.
11. A. I. El-Batal, F. M. Mosallam, and G. S. El-Sayyad (2018). *J. Cluster Sci.* **29**, (6), 1003–1015.
12. G. Carotenuto, Y.-S. Her, and E. Matijević (1996). *Ind. Eng. Chem. Res.* **35**, (9), 2929–2932.
13. C. Sanchez, F. Ribot, and B. Lebeau (1999). *J. Mater. Chem.* **9**, (1), 35–44.
14. T. Morsi, A. M. Elbarbary, M. M. Ghobashy, and S. H. Othman (2018). *Radiochim. Acta* **106**, (5), 383–392.
15. M. G. Naseri, E. B. Saion, H. A. Ahangar, and A. H. Shaari (2013). *Mater. Res. Bull.* **48**, (4), 1439–1446.
16. E. Hao, S. Li, R. C. Bailey, S. Zou, G. C. Schatz, and J. T. Hupp (2004). *J. Phys. Chem. B* **108**, (4), 1224–1229.
17. C. Salzemann, I. Lisiecki, A. Brioude, J. Urban, and M.-P. Pileni (2004). *J. Phys. Chem. B* **108**, (35), 13242–13248.
18. S. Sagadevan, K. Pal, Z. Z. Chowdhury, and M. E. Hoque (2017). *J. Sol–Gel Sci. Technol.* **83**, (2), 394–404.
19. A. El-Batal, B. M. Haroun, A. A. Farrag, A. Baraka, and G. S. El-Sayyad (2014). *Br. J. Pharm. Res.* **4**, (11), 1341.
20. A. I. El-Batal, N. E. Al-Hazmi, F. M. Mosallam, and G. S. El-Sayyad (2018). *Microb. Pathog.* **118**, 159–169.
21. A. I. El-Batal, N. M. Sidkey, A. Ismail, R. A. Arafa, and R. M. Fathy (2016). *J. Chem. Pharm. Res* **8**, (4), 934–951.
22. G. S. El-Sayyad, F. M. Mosallam, and A. I. El-Batal (2018). *Adv. Powder Technol.* **29**, (11), 2616–2625.
23. F. M. Mosallam, G. S. El-Sayyad, R. M. Fathy, and A. I. El-Batal (2018). *Microb. Pathog.* **122**, 108–116.
24. J. Li, B. Kang, S. Chang, and Y. Dai (2012). *Micro Nano Lett.* **7**, (4), 360–362.
25. A. I. El-Batal, G. S. El-Sayyad, A. El-Ghamery, and M. Gobara (2017). *J. Cluster Sci.* **28**, (3), 1083–1112.
26. A. I. El-Batal, F. M. Mosalam, M. Ghorab, A. Hanora, and A. M. Elbarbary (2018). *Int. J. Biol. Macromol.* **107**, 2298–2311.
27. A. F. El-Baz, A. I. El-Batal, F. M. Abomosalam, A. A. Tayel, Y. M. Shetaia, and S. T. Yang (2016). *J. Basic Microbiol.* **56**, (5), 531–540.
28. A. I. El-Batal, G. S. El-Sayyad, A. El-Ghamry, K. M. Agaypi, M. A. Elsayed, and M. Gobara (2017). *J. Photochem. Photobiol., B* **173**, 120–139.
29. T. Thirugnanasambandan, K. Pal, A. Sidhu, M. A. Elkodous, H. Prasath, K. Kulasekarapandian, A. Ayeshamariam, and J. Jeevanandam (2018). *Nano-Struct. Nano-Objects* **16**, 224–233.
30. A.-W. A. Ismail, N. M. Sidkey, R. A. Arafa, R. M. Fathy, and A. I. El-Batal (2016). *Br. Biotechnol. J.* **12**, (3), 1.
31. K. F. Abdellatif, R. H. Abdelfattah, and M. S. M. El-Ansary (2016). *Iran. J. Biotechnol.* **14**, (4), 250.
32. W. Cromwell, J. Yang, J. Starr, and Y.-K. Jo (2014). *J. Nematol.* **46**, (3), 261.
33. S. Davarpanah, A. Tehranifar, G. Davarynejad, J. Abadía, and R. Khorasani (2016). *Sci. Hortic.* **210**, 57–64.
34. I. A. Jehangir, S. H. Wani, M. A. Bhat, A. Hussain, W. Raja, and A. Haribhushan (2017). *Int. J. Curr. Microbiol. App. Sci.* **6**, (11), 5347–5353.
35. P. Brown, N. Bellaloui, M. Wimmer, E. Bassil, J. Ruiz, H. Hu, H. Pfeffer, F. Dannel, and V. Römheld (2002). *Plant Biol.* **4**, (02), 205–223.
36. E. A. A. Couto, C. R. Dias-Arieira, J. Kath, J. A. Homiak, and H. H. Puerari (2016). *Acta Agric. Scand., Sect. B—Soil Plant Sci.* **66**, (4), 346–352.
37. S. Sajjadifar, K. Pal, H. Jabbari, O. Pouralimardan, F. Divsar, S. Mohammadi-Aghdam, I. Amini, and H. Hamidi (2019). *Chem. Methodol.* **3**, (2. pp. 145–275), 226–236.
38. D. H. D. Silva, M. L. Rossi, A. E. Boaretto, N. D. L. Nogueira, and T. Muraoka (2008). *Scientia Agricola* **65**, (6), 659–664.
39. A. Taylor and J. Sasser, Biology, Identification and Control of Root-Knot Nematodes (North Carolina State University Graphics, 1978), p. 111.
40. K. Barker and R. Hussey (1976). *Phytopathology* **66**, (7), 851–855.
41. K. Brownlee *Probit Analysis: A Statistical Treatment of the Sigmoid Response Curve* (JSTOR, New York, 1952).
42. F.-K. Liu, Y.-C. Hsu, M.-H. Tsai, and T.-C. Chu (2007). *Mater. Lett.* **61**, (11–12), 2402–2405.
43. M. Składanowski, M. Wypij, D. Laskowski, P. Golińska, H. Dahm, and M. Rai (2017). *J. Cluster Sci.* **28**, (1), 59–79.
44. O. Borokhov and D. Schubert *Antimicrobial Properties of Boron Derivatives, ACS Symposium Series* (Oxford University Press, Oxford, 2007), pp. 412–435.
45. R. Scott, A. J. Veinot, D. Stack, P. Gormley, N. Khuong, C. M. Vogels, J. D. Masuda, F. Baerlocher, T. MacCormack, and S. A. Westcott (2018). *Can. J. Chem.* **96**, 906–911.
46. W. Yuzheng, X. Xiangxin, and Y. He (2014). *Chin. J. Chem. Eng.* **22**, (4), 474–479.
47. A. Ashour, A. I. El-Batal, M. A. Maksoud, G. S. El-Sayyad, S. Labib, E. Abdeltwab, and M. El-Okr (2018). *Particuology* **40**, 141–151.
48. M. A. Maksoud, G. S. El-Sayyad, A. Ashour, A. I. El-Batal, M. A. Elsayed, M. Gobara, A. M. El-Khawaga, E. Abdel-Khalek, and M. El-Okr (2019). *Microb. Pathog.* **127**, 144–158.
49. M. G. Naseri, E. Saion, and N. K. Zadeh (2013). *Int. Nano Lett.* **3**, (1), 19.
50. R. Bryaskova, D. Pencheva, S. Nikolov, and T. Kantardjiev (2011). *J. Chem. Biol.* **4**, (4), 185.
51. M. A. Maksoud, A. El-ghandour, G. S. El-Sayyad, A. Awed, R. A. Fahim, M. Atta, A. Ashour, A. I. El-Batal, M. Gobara, and E. Abdel-Khalek (2019). *J. Mater. Sci.: Mater. Electron.*. https://doi.org/10.1007/s10854-019-00785-4.
52. A. Gannoruwa, B. Ariyasinghe, and J. Bandara (2016). *Catal. Sci. Technol.* **6**, (2), 479–487.
53. K. Kumar, M. Ravi, Y. Pavani, S. Bhavani, A. Sharma, and V. V. R. Narasimha Rao (2012). *J. Non-Cryst. Solids* **358**, (23), 3205–3211.
54. K. K. Kumar, M. Ravi, Y. Pavani, S. Bhavani, A. Sharma, and V. N. Rao (2014). *J. Membr. Sci.* **454**, 200–211.
55. N. F. Himma, A. K. Wardani, N. Prasetya, P. T. Aryanti, and I. G. Wenten. Rev. Chem. Eng.
56. W. H. Eisa, Y. K. Abdel-Moneam, Y. Shaaban, A. A. Abdel-Fattah, and A. M. A. Zeid (2011). *Mater. Chem. Phys.* **128**, (1–2), 109–113.
57. K. N. Kumar, K. Sivaiah, and S. Buddhudu (2014). *J. Lumin.* **147**, 316–323.

58. A. Abdelghany, E. Abdelrazek, and D. Rashad (2014). *Spectrochim. Acta A Mol. Biomol. Spectrosc.* **130**, 302–308.
59. S. Selvasekarapandian, R. Baskaran, O. Kamishima, J. Kawamura, and T. Hattori (2006). *Spectrochim. Acta A Mol. Biomol. Spectrosc.* **65**, (5), 1234–1240.
60. E. Abdelrazek, A. Abdelghany, S. Badr, and M. Morsi (2016). *Res. J. Pharm. Biol. Chem. Sci.* **7**, 1877–1890.
61. A. Abdelghany, E. Abdelrazek, S. Badr, and M. Morsi (2016). *Mater. Des.* **97**, 532–543.
62. P.-Y. Silvert, R. Herrera-Urbina, and K. Tekaia-Elhsissen (1997). *J. Mater. Chem.* **7**, (2), 293–299.
63. B. Sadeghi, M. Sadjadi, and A. Pourahmad (2008). *Int. J. Nanosci. Nanotechnol.* **4**, (1), 3–12.
64. Z. Zhang, B. Zhao, and L. Hu (1996). *J. Solid State Chem.* **121**, (1), 105–110.
65. Y. Wang and H. Wang (2009). *Radiat. Phys. Chem.* **78**, (3), 234–237.
66. A. I. El-Batal, A. A. Farrag, M. A. Elsayed, and A. M. El-Khawaga (2016). *Bioengineering* **3**, (2), 14.
67. A. I. El-Batal, F. A. E.-L. Gharib, S. M. Ghazi, and A. Z. Hegazi (2016). *Nanomater. Nanotechnol.* **6**, 13.
68. A. Hanora, M. Ghorab, A. I. El-Batal, and F. M. A. Mosalam (2016). *J. Chem. Pharm. Res.* **8**, (3), 405–423.
69. H. Abou-Aly, R. Zaghloul, N. Neweigy, S. El-Sayed and A. Bahloul, Suppression of Root-Knot Nematode (*Meloidogyne incognita*) Activity in Tomato Using Biocontrol Agents, The 2nd Minia International Conference (Agriculture and Irrigation in Nile Basin Countries, 2015), pp. 23–25.
70. U.D.o. Health, H. Services, Toxicological Profile for Silver, TP-90-24. Atlanta, GA (1990).
71. Y. M. Amin, A. M. Hawas, A. El-Batal, and S. H. H. E. Elsayed (2015). *Br. J. Pharmacol. Toxicol.* **6**, (2), 22–38.
72. M.-C. Caillaud, P. Lecomte, F. Jammes, M. Quentin, S. Pagnotta, E. Andrio, J. de Almeida Engler, N. Marfaing, P. Gounon, and P. Abad (2008). *Plant Cell* **20**, (2), 423–437.
73. A.C. Baier, Regulating Nanosilver as a Pesticide, Environmental Defense Fund, February 12 (2009).
74. D. Lim, J. Y. Roh, H. J. Eom, J. Y. Choi, J. Hyun, and J. Choi (2012). *Environ. Toxicol. Chem.* **31**, (3), 585–592.
75. H.-J. Park, S.-H. Kim, H.-J. Kim, and S.-H. Choi (2006). *Plant Pathol. J.* **22**, (3), 295–302.
76. Y.-K. Jo, B. H. Kim, and G. Jung (2009). *Plant Dis.* **93**, (10), 1037–1043.
77. P. Beyli, M. Doğan, Z. Gündüz, M. Alkan, and Y. Turhan (2018). *Adv. Mater. Sci.* **18**, (1), 28–36.
78. W. Akbar, M. R. Noor, K. Kowal, T. Syed, T. Soulimane, and G. B. Basim (2017). *Adv. Powder Technol.* **28**, (2), 596–610.
79. D. G. Blevins and K. M. Lukaszewski (1998). *Annu. Rev. Plant Biol.* **49**, (1), 481–500.
80. F. Shireen, M. Nawaz, C. Chen, Q. Zhang, Z. Zheng, H. Sohail, J. Sun, H. Cao, Y. Huang, and Z. Bie (2018). *Int. J. Mol. Sci.* **19**, (7), 1856.
81. M. A. Beni, A. Hatamzadeh, A. Nikbakht, M. Ghasemnezhad, and M. Zarchini (2013). J. Ornam. Hortic. Plants, 3(3).
82. H. M. Salama (2012). *Int. Res. J. Biotechnol.* **3**, (10), 190–197.
83. V. Ramamoorthy, R. Viswanathan, T. Raguchander, V. Prakasam, and R. Samiyappan (2001). *Crop Prot.* **20**, (1), 1–11.
84. D. Walters, A. Newton, and G. Lyon *Induced Resistance for Plant Defence* (Wiley Online Library, Hoboken, 2007).
85. N. Wuyts, D. De Waele, and R. Swennen (2006). *Plant Physiol. Biochem.* **44**, (5–6), 308–314.
86. N. Sudhakar, D. Nagendra-Prasad, N. Mohan, and K. Murugesan (2007). *J. Virol. Methods* **139**, (1), 71–77.
87. I. Morkunas and J. Gmerek (2007). *J. Plant Physiol.* **164**, (2), 185–194.
88. N. Strigul, L. Vaccari, C. Galdun, M. Wazne, X. Liu, C. Christodoulatos, and K. Jasinkiewicz (2009). *Desalination* **248**, (1–3), 771–782.